Presented at the 1998 Applied Superconductivity Conference,
September 14 - 18, 1998, Palm Desert, CA

Simultaneous Optimization of the Linear and Nonlinear Microwave Response of YBCO Films and Devices

James C. Booth, J. A. Beall, D. A. Rudman, L. R. Vale, and R. H. Ono
National Institute of Standards and Technology, Boulder, Colorado, 80303, U.S.A.

C. L. Holloway
Institute for Telecommunication Sciences/NTIA, 325 Broadway, Boulder, CO 80303, U.S.A.

S. B. Qadri, M. S. Osofsky, E. F. Skelton, and J. H. Claassen
Naval Research Laboratory, Washington, D.C., U.S.A.

G. Gibson, J. L. MacManus-Driscoll, N. Malde and L. F. Cohen
Centre for Superconductivity, Blackett Laboratory, Imperial College, London, UK

***Abstract* – We present results of a systematic study of the effect of film deposition temperature on both the linear and nonlinear response of superconducting $YBa_2Cu_3O_{7-\delta}$ (YBCO) thin films and devices at microwave frequencies. Measurements of the unpatterned films show that samples grown by pulsed laser deposition at a lower substrate temperature (740 ˚C) display a smaller low-temperature residual surface resistance compared to films grown at a higher substrate temperature (780 ˚C). However, the same films which display low residual surface resistance also show increased nonlinear effects (measured by third harmonic generation) at all temperatures. Analysis of these results suggests that the increased defects present in the films grown at the lower deposition temperature are responsible for both the lower surface resistance and the higher third harmonic generation observed in these samples. We discuss the consequences of these results for the simultaneous optimization of both linear and nonlinear microwave properties of HTS thin films and devices.**

I. Introduction

One of the first areas of practical application for high temperature superconductor (HTS) devices is passive microwave circuits [1]-[3]. In order to maximize device performance, much effort has been expended in learning how to fabricate HTS materials with very low surface resistance[1]. In addition to low microwave loss, however, HTS materials can exhibit detrimental nonlinear behavior at microwave frequencies [4,5]. It is becoming increasingly apparent, for some applications at least (such as transmit and receive filters), that it is desirable to fabricate devices that have both low nonlinearity and low microwave loss. Since the origins of nonlinearity in HTS devices are not well understood, it is not immediately obvious if the same film growth conditions that lead to low surface resistance will also produce low nonlinearity. In the case of single crystals of $YBa_2Cu_3O_{7-\delta}$ (YBCO), for example, increasing concentrations of certain types of impurities produces a lower surface resistance [6]. While the effect of such impurities on the nonlinear response is unknown, it is certainly possible that factors which lead to the lowest surface resistance could result in increased nonlinear effects.

In this paper we present results of a systematic study of the effect of film deposition temperature on both the linear and nonlinear microwave response of HTS materials fabricated by pulsed-laser deposition (PLD). This study is not intended to be a comprehensive survey of all possible film deposition conditions, but is rather meant as an initial effort at the simultaneous optimization of linear and nonlinear microwave properties of HTS thin films. We find evidence that the increase in defects resulting from film growth at lower deposition temperatures leads to a smaller low-temperature surface resistance (R_s) and also gives rise to a larger nonlinear response. These results point to the need for detailed study of the effects of different kinds of defects and disorder on the surface resistance and nonlinearity, in order to develop films and devices optimized for both low surface resistance and low nonlinearity.

II. Film Deposition/Characterization

We have grown a series of 18 YBCO thin films by pulsed laser deposition on $LaAlO_3$ substrates while systematically varying the film deposition temperature between 740 ˚C and 790 ˚C [7], holding the oxygen pressure during deposition constant at 68 Pa (500 mTorr). From this series we select four films grown at 740 ˚C and four films grown at 780 ˚C for detailed evaluation. The films are 15 mm x 15 mm in area, and are all nominally 400 nm thick. Films grown at 780 ˚C have an inductive T_c (onset) of 90.5 K to 90.9 K, whereas the samples grown at 740 ˚C have an inductive T_c approximately 0.5 to 1 K lower than the 780 ˚C films. Inductive measurements give similar values for the critical current density at 76 K (J_c = 3.2 to 3.5 x 10^6 A/cm^2) for both the 740 ˚C and 780 ˚C films. Scanning electron microscope (SEM) images show a roughly constant density of surface

Manuscript received September 15, 1998.

This work supported in part by the Office of Naval Research; the contribution of J.C.B. was supported by a NIST/NRC Postdoctoral Research Associateship.

outgrowths ("boulders") for all films, but the films grown at lower deposition temperature show a significantly larger density of growth islands than films deposited at higher temperatures, which is consistent with earlier observations [8]. In addition to producing a larger density of growth islands, the lower deposition temperature is generally thought to incorporate more defects into the film as it grows [8]. The motivation for varying the film deposition temperature in this study is therefore to investigate the effect of these kinds of defects on both the linear and nonlinear electrodynamic properties of these materials at microwave frequencies.

In addition to the standard characterization described above, we also select representative samples grown at 740 ˚C and 780 ˚C for further microstructural analysis, which includes Raman spectroscopy measurements [9], and high resolution x-ray diffraction measurements [10]. Raman spectroscopy measurements on the 740 ˚C and 780 ˚C samples show that both sets of films have similar levels of cation disorder (approximately 2-3%), and similar low levels of a-axis coverage. The x-ray measurements are performed using a diffractometer which has a very high angular resolution of approximately 0.0025 degree [10]. The c–axis lattice parameter is determined to be 1.168 nm for all samples, indicative of fully oxygenated YBCO material. In addition, the x-ray measurements show no evidence for a-axis growth down to the resolution limit of the instrument, estimated to be < 2%. (The presence of a-axis growth is inferred from the presence of the (200) peak in the θ-2θ scans.) These measurements reveal little structural difference between samples grown at different deposition temperatures, but reinforce the conclusion that all the films investigated are structurally good.

III. Unpatterned Microwave Measurements

We measure the surface resistance at 76 K of all films using a sapphire dielectric resonator operating at 17.5 GHz [11] and obtain values in the range 0.8 to 1.3 mΩ (which gives 0.26 to 0.42 mΩ when scaled by f^2 to 10 GHz). We find that the surface resistance at 76 K increases slightly for the films grown at lower deposition temperatures. For the 740 ˚C and 780 ˚C sets of films we also measure the microwave loss as a function of temperature, shown in Fig. 1. These measurements illustrate that at low measurement temperature the 740 ˚C films have a significantly lower surface resistance than the 780 ˚C films, resulting in a higher (unloaded) resonator quality factor. This behavior is also displayed in the inset of Fig. 1, which shows values for R_s at 17.5 GHz extracted from the dielectric resonator measurements.

To further investigate the difference in microwave response of our YBCO films grown at different deposition temperatures, we extract from our temperature-dependent R_s measurements the real and imaginary parts of the complex conductivity ($\sigma = \sigma_1 + i\,\sigma_2$), which are shown in Fig. 2. This is accomplished by combining the temperature-dependent measurements of the quality factor and frequency shift of our dielectric resonator with measurements of the penetration depth at 77 K [12] on representative samples. Note that the films grown at lower deposition temperature exhibit a smaller value of σ_1 than the samples grown at 780 ˚C over the entire temperature range. (The smaller σ_1 could result from a higher quasiparticle scattering rate, since the quasiparticle scattering rate is inversely proportional to σ_1.) A higher scattering rate is consistent with the lower film deposition temperature producing films having more defects. In addition to a reduced σ_1, the lower deposition temperature also gives a smaller value of σ_2, which is an indication of a smaller superconducting carrier density (or equivalently, a larger penetration depth). Although the decreased σ_1 produces a lower surface resistance at low temperature, by 76 K the effect of the lower carrier density (larger penetration depth) has caused the surface resistance of the 740 ˚C samples to increase above the surface resistance for the 780 ˚C samples. This results in the cross-over at approximately 70 K in the temperature dependence of the dielectric resonator quality factor (and hence also in the surface resistance) illustrated in Fig. 1.

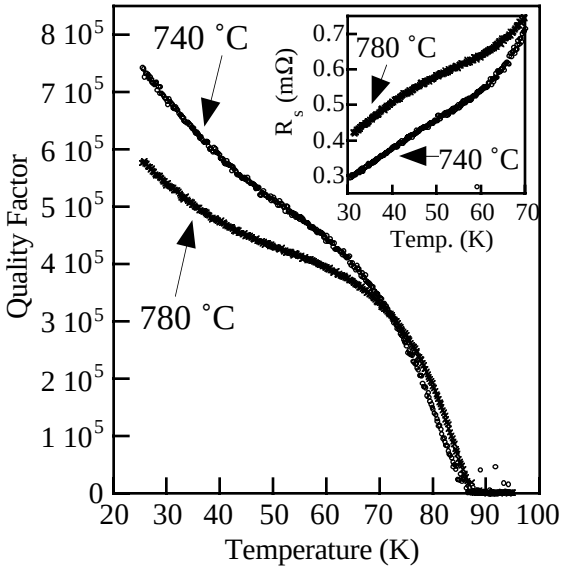

Fig. 1. Temperature dependence of sapphire dielectric resonator quality factor for pairs of YBCO films grown at deposition temperatures of 780 ˚C and 740 ˚C. The inset shows values for the surface resistance at 17.5 GHz extracted from the dielectric resonator measurements.

IV. Device Fabrication and Characterization

In order to facilitate measurement of the nonlinearity in our YBCO thin films at microwave frequencies, we pattern our samples into coplanar waveguide (CPW) transmission lines of varying dimensions using standard photolithography and Ar ion milling. We pattern many different CPW devices on a single YBCO chip in order to verify that our measurements yield the intrinsic material properties of the superconductor, rather than possible measurement or device-related artifacts. Both linear and nonlinear microwave measurements are performed using a vector network analyzer and a cryogenic microwave probe station, which allows for the characterization

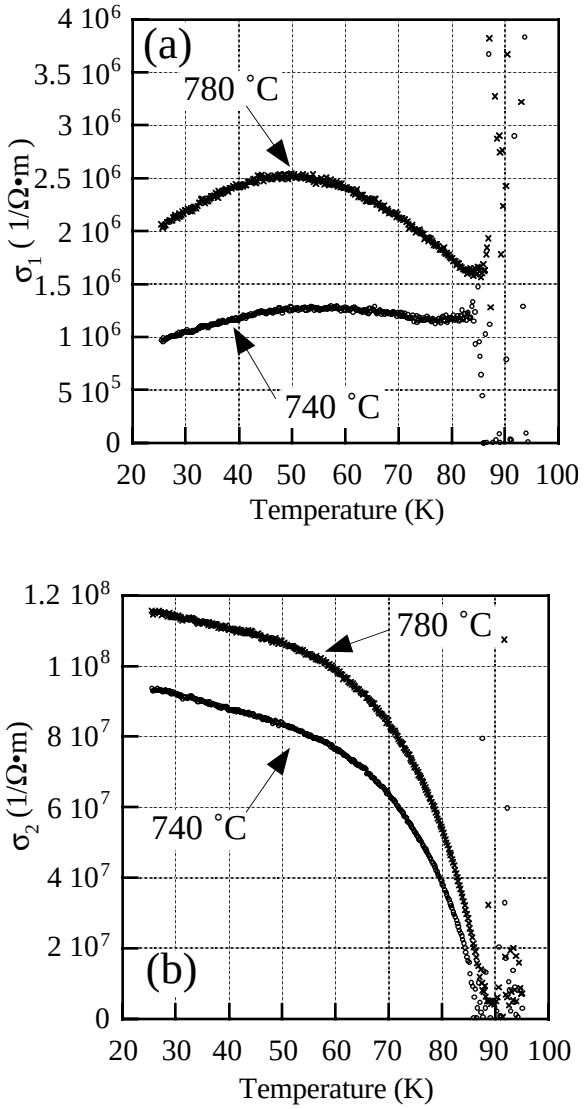

Fig. 2. Temperature dependence of (a) the real part of the complex conductivity σ_1 and (b) the imaginary part of the complex conductivity σ_2 for YBCO films deposited at 740 ˚C and 780 ˚C.

of many individual devices on a given chip during a single cool-down. Gold contacts are evaporated onto the CPW devices to ensure good electrical contact between the movable microwave probes and the patterned devices. More details of device fabrication and cryogenic probe station measurements can be found in [13], [14].

To make certain that the superconducting material has not changed or degraded during device fabrication, we measure the quality factor as a function of temperature for patterned CPW resonators of length 11.35 mm and width 21 µm, which have a fundamental resonant frequency of 3.7 GHz. The results of these measurements, shown as points in Fig. 3, confirm that the patterned structures display the same qualitative shape as observed in the unpatterned measurements, with the 740 ˚C samples having a higher quality factor than the 780 ˚C samples at low temperatures. To further verify that

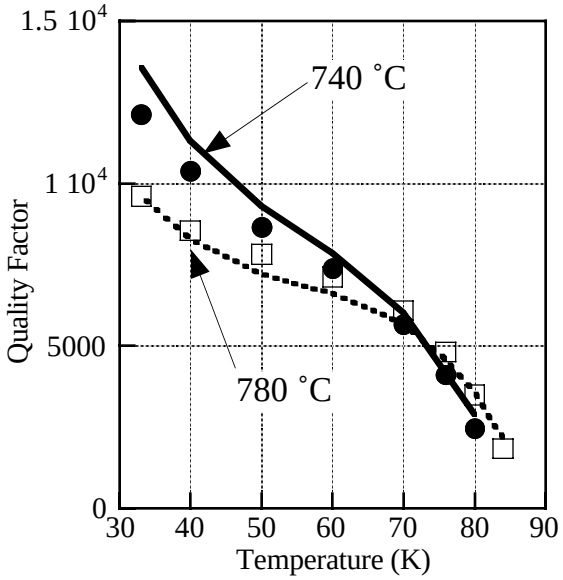

Fig. 3. Quality factor for patterned CPW resonators vs. temperature, fabricated from YBCO films grown at 740 ˚C and 780 ˚C. The individual points represent Q measurement for a 21 µm wide, 11.35 mm long CPW resonator at its fundamental frequency of 3.7 GHz. The solid lines are theoretical values for the quality factor based on a model calculation using the measurement data for the unpatterned films shown in Figs. 1 and 2.

our CPW devices are operating as expected, we use a theoretical calculation of the phase and attenuation constant for superconducting planar devices [15] to calculate the expected quality factor for the CPW resonators. We use as input to the calculation the temperature dependent data for the surface resistance and penetration depth measured on the unpatterned samples, and obtain results which are shown as the solid and dashed lines in Fig. 3. Overall, we can conclude from these resonator measurements that our patterned CPW lines are operating exactly as expected from our unpatterned measurements.

V. Nonlinear Measurements

We characterize the nonlinear response of our superconducting samples using third harmonic generation measurements as a function of microwave power in patterned CPW transmission lines. This technique detects the third harmonic signal generated by nonlinearities in our system as a function of incident microwave power. We use a network analyzer in continuous wave (CW) mode as a source to provide a single tone signal at a frequency of 3 GHz. This signal is fed into a solid-state amplifier and then through a low-pass filter (which removes unwanted harmonics generated by the source and amplifier), and then into the cryogenic probe station containing our superconducting transmission lines. The fundamental signal and any generated harmonics are sampled at the output of the probe station using a 20 dB directional coupler connected to a spectrum analyzer, while the main signal path is terminated in a high power 50 Ω load.

The results of such a measurement of third harmonic generation as a function of incident power are shown in Fig. 4.

(The units of power quoted are decibels referenced to 1 mW, abbreviated dBm.) For nonlinearities that are small, we expect the magnitude of the third harmonic to increase with the third power of the incident signal. This yields a slope of 3 for the third harmonic signal when viewed on a log-log plot, as illustrated in Fig. 4. We obtain this type of behavior for almost all of the devices that we measure. We adopt the convention to specify the nonlinearity in a specific circuit by quoting the third-order intercept P_{TOI}, which is defined as the point at which the magnitude of the third harmonic would become equal to the magnitude in the fundamental (see Fig. 4). In practice, the critical current density of the superconductor is exceeded well before this power is reached. However, the third-order intercept is still a useful figure of merit for specifying the nonlinearity associated with a given component.

We expect the simple "slope 3" behavior of the third harmonic signal described above to be valid as long as the nonlinearity can be considered small. If we drive the system at high enough power, this small-signal approximation begins to break down. Such a case is illustrated in the inset of Fig. 4, where the detected power in the third harmonic begins to saturate at high incident power. In defining an accurate value for the third-order intercept, it is important to exclude such regions where the assumptions of a small third harmonic signal are no longer valid.

Having defined the third-order intercept as a quantitative measure of nonlinearity for a given HTS device, we need a way to relate third-order intercepts for devices having different physical dimensions in order to make useful comparisons of nonlinearity among different samples. We have developed a method, described in another publication [16], which allows the third-order intercept to be transformed to take into account different device geometries, such as center conductor line width, line length, and film thickness. We accomplish this by scaling the measured P_{TOI} for different geometry samples to a standard reference geometry [17]. In this manner we can quantitatively compare the nonlinear response of different samples even if the specific device geometry is different. In addition, we have also reported that the measured third-order intercepts for our CPW devices are relatively insensitive to the details of the device fabrication process. These two experimental conclusions combine to give us a powerful tool for determining the intrinsic material nonlinearities present in our samples.

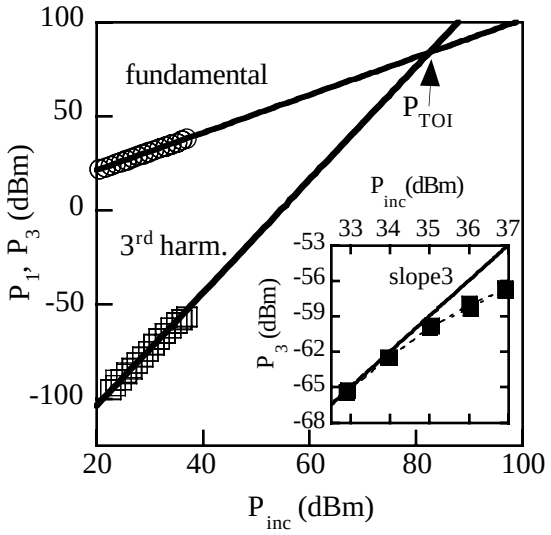

Fig. 4. Measured power in the fundamental (P_1) and third harmonic (P_3) as a function of incident power. Solid lines are fits of slope 1 for the fundamental and slope 3 for the third harmonic. The intersection of these two lines defines the third-order intercept. Inset: example of deviation from slope three of third harmonic signal that occurs for high incident powers.

Fig. 5(a) shows the measured third-order intercepts as a function of temperature for several different samples scaled in the manner described above[17]. The samples grown at 740 ˚C have lower values of P_{TOI} (indicating more nonlinearity) than the 780 ˚C samples over the entire temperature range. This higher nonlinearity is in contrast to the results of our surface resistance measurements for both the unpatterned films and the patterned devices, which show better performance for the 740 ˚C samples over much of the investigated temperature range. Reference to Fig. 2 suggests two possible reasons for the higher nonlinearity observed in the 740 ˚C samples: the 740 ˚C samples have a lower value of σ_1 (implying perhaps a higher quasiparticle scattering rate), and a smaller superconducting carrier density (or equivalently a larger superconducting penetration depth). It is likely that both of these factors contribute to the increased nonlinearity observed in the 740 ˚C samples.

To further investigate the origins of the observed differences in nonlinear response, we use a simple model [16,18] that relates third harmonic generation to an intrinsic material parameter, the nonlinear scaling current density J_0. This model assumes a nonlinear inductance term in the characteristic transmission line equations, which arises from a current-dependent magnetic penetration depth. In this analysis, the third-order intercepts depend explicitly on the penetration depth. This model has been used to successfully describe the observed geometry dependence for a large number of CPW devices, yielding the geometry-independent parameter J_0 to quantify the observed nonlinearity [16]. We use this model to calculate the temperature dependence of the nonlinear current density J_0 in order to eliminate the intrinsic penetration depth dependence of the measured third-order intercept P_{TOI}. The resulting values of J_0 as a function of temperature are plotted in Fig. 5(b) for the 740 ˚C and 780 ˚C samples. This figure shows that the 740 ˚C samples still display more nonlinearity (as evidenced by the lower value for J_0) than the 780 ˚C samples, even after the larger penetration depth has been taken into account. This suggests that the remaining difference in J_0 may be related to differences in the real part of the conductivity σ_1. If this is the case, then the quasiparticle scattering may be at least partly responsible for both the lower R_s and lower J_0 observed in the more disordered 740 ˚C samples.

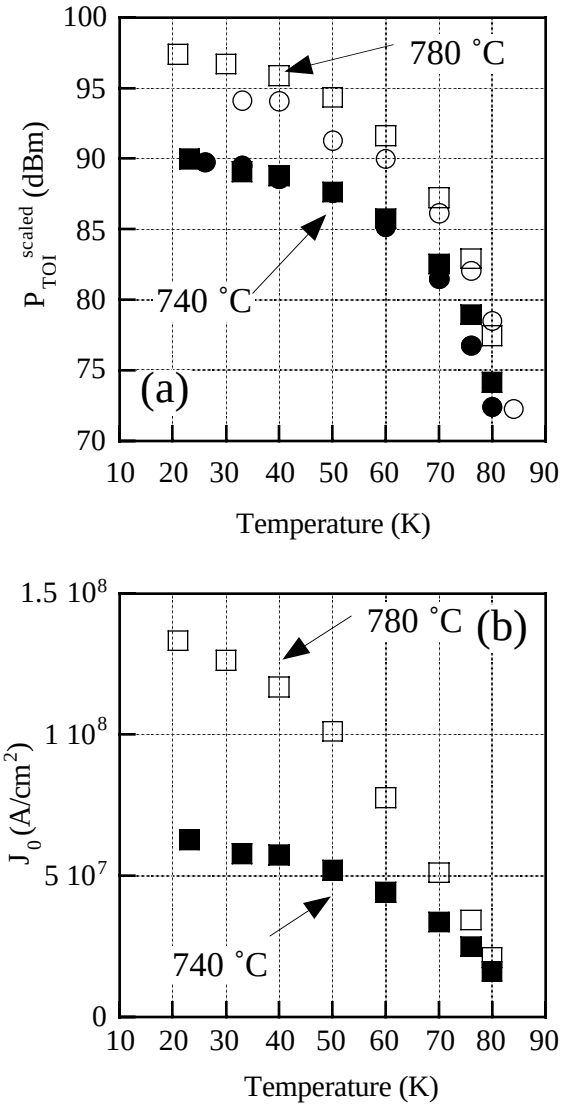

Fig. 5. Temperature dependence of (a) the scaled third-order intercept and (b) the nonlinear scaling current density J_0 for films grown at deposition temperatures of 740 ˚C and 780 ˚C.

Such a common origin is also suggested by the fact that the ratio of J_0 at low temperatures of the 740 ˚C and 780 ˚C samples (approximately a ratio of 2) is roughly the same as the ratio of the real part of the conductivity σ_1 for the samples at low temperatures; see Fig. 2(a).

CONCLUSIONS

We have systematically explored the effect of varying the film deposition temperature on both the linear and nonlinear microwave response of HTS films and devices fabricated by pulsed-laser deposition. Our measurements suggest that the increased defects present in films grown at lower deposition temperatures are responsible at least in part for both the lower surface resistance and also the higher nonlinearity observed in these samples. Further microstructural analysis is necessary to understand the nature of the defects present in these samples. In order to develop a viable process to produce films with simultaneous low R_s and high P_{TOI}, it is necessary to find methods by which to decrease the real part of the conductivity (to achieve low R_s) without adversely affecting either the penetration depth or the nonlinear scaling current density J_0. These results illustrate the necessity of investigating the effects of different kinds of defects and disorder on both the surface resistance and nonlinearity in order to develop a process for simultaneously optimizing both the linear and nonlinear properties of HTS films and devices.

REFERENCES

[1] Z. Y. Shen, *High-Temperature Superconducting Microwave Circuits* . Artech House: Boston, 1994.

[2] N. Newman and W. G. Lyons, "High-temperature superconducting microwave devices: fundamental issues in materials, physics, and engineering," *J. Supercond*., Vol. 6, 1993, pp. 119-160.

[3] J. Gallop, "Microwave application of high-temperature superconductors," *Supercond. Sci. Technol.* Vol. 10, 1997, pp. A120-A141.

[4] D. E. Oates, P.P. Nguyen, G. Dresselhaus, M.S. Dresselhaus, C.W. Lam, and S.M. Ali, "Measurements and modeling of linear and nonlinear effects in striplines," *J. Supercond*., Vol. 5, 1992, pp. 361-369.

[5] C. Wilker, Z. Y. Shen, P. Pang, W. L. Holstein, and D. W. Face, "Nonlinear effects in high temperature superconductors: 3rd order intercept from harmonic measurements," *IEEE Trans. Appl. Supercond.* Vol. 5, 1995, pp.1665-1670.

[6] D.A. Bonn, S. Kamal, K. Zhang, D.J. Baar, E. Klein, and W.N. Hardy, "Comparison of the influence of Ni and Zn impurities on the electromagnetic properties of $YBa_2Cu_3O_{6.95}$," Phys. Rev. B Vol. 50, 1994, pp. 4015-4063.

[7] The quoted temperature is that of the heater block. The actual substrate temperature during deposition may be 50 to 70 ˚C less.

[8] A. Roshko, F. J. B. Stork, D. A. Rudman, D. J. Aldrich, P. A. Morris Hotsenpiller, "Comparison of heteroepitaxial $YBa_2Cu_3O_{7-\delta}$ and TiO_2 thin film growth," *J. Crystal Growth*, Vol. 174, 1997, pp. 398-408.

[9] G. Gibson, J. L. MacManus-Driscoll, and L. F. Cohen, "Raman microscopy as a local probe of structural defects and oxygen content in HTS thin films," *IEEE Trans. Appl. Supercond.* Vol. 7, 1997, pp. 2130-2133.

[10] B. M. Browning, E.F. Skelton, M.S. Osofsky, S.B. Qadri, J.Z. Ju, L.W. Finger, and P. Caubet, "Structural inhomogeneities observed in $YBa_2Cu_3O_{7-\delta}$ crystals with optimal transport properties," *Phys. Rev. B*, Vol. 56, 1997, pp. 2860-2870.

[11] F. J. B. Stork, J.A. Beall, A. Roshko, D.C. DeGroot, D.A. Rudman, and R.H. Ono, "Surface resistance and morphology of YBCO films as a function of thickness," *IEEE Trans. Appl. Supercond.* Vol. **7**, 1997, pp. 1921-1924.

[12] J. H. Claassen, M.L. Wilson, J.M. Byers, and S. Adrian, "Optimizing the two-coil mutual inductance measurement of the superconducting penetration depth in thin films," *J. Appl. Phys.* Vol. 82, 1997, pp. 3028-3034.

[13] J. C. Booth, J.A. Beall, D.C. DeGroot, D.A. Rudman, R.H. Ono, J.R. Miller, M.L. Chen, S.H. Hong, and Q.Y. Ma, "Microwave characterization of coplanar waveguide transmission lines fabricated by ion implantation patterning of $YBa_2Cu_3O_{7-\delta}$," *IEEE Trans. Appl. Supercond.* Vol. 7, 1997, pp. 2780-2783.

[14] James C. Booth, J.A. Beall, R.H. Ono, F.J.B. Stork, D.A. Rudman, and L.R. Vale, "Third-order harmonic generation in high-temperature superconducting coplanar waveguides at microwave frequencies," *Appl. Supercond.* Vol. 5, 1998, pp. 379-384.

[15] James C. Booth and Christopher L. Holloway, "Conductor loss in superconducting planar structures: Calculation and measurements," unpublished.

[16] James C. Booth, J. A. Beall, D. A. Rudman, L. R. Vale, and R. H. Ono, "Geometry dependence of nonlinearities in high temperature superconducting transmission lines at microwave frequencies," unpublished.

[17] For the data reported here, we scale the third-order intercept to a reference geometry of length 10 mm, center conductor linewidth 100 µm, and thickness 500 nm.

[18] T. Dahm and D.J. Scalapino, "Theory of intermodulation in a superconducting microstrip resonator," J. Appl. Phys. Vol. 81, 1997, pp. 2002 - 2009.